UDC 551.584.5:551.588.7:551.556

THEORETICAL ANALYSIS OF THE EFFECT OF MEAN WIND AND STABILITY ON A HEAT ISLAND CIRCULATION CHARACTERISTIC OF AN URBAN COMPLEX

FRED M. VUKOVICH

Engineering and Environmental Sciences Division, Research Triangle Institute, Research Triangle Park, N.C.

ABSTRACT

A simple two-dimensional linear model was used to explore the nature of the heat island circulation of an urban area. Two stability categories, stable and near-neutral, were assumed to define the boundary layer conditions. The heat island circulation was studied under the condition of no-mean wind and also for cases when a mean wind existed. The forcing function (differential heating) was given as a smoothly varying function in the horizontal that would create a smoothly varying temperature field with no discontinuities in the temperature distribution. A rather weak two-cell circulation system was developed in which depth and intensity were dependent on the boundary layer stability. Allowing a mean wind to exist produced a displacement of the two-cell circulation downstream to a location that is a function of the heating rate and the advection of heat and momentum by the mean wind.

1. INTRODUCTION

An urban complex acts as a heat reservoir producing a positive perturbation on the thermal field. This perturbation is called "the urban heat island" (Lowry 1967, Mitchell 1961, Clarke 1969). The horizontal temperature pattern associated with the heat island is a function of the urban terrain. For instance, the temperature differences between structure areas and parks are significant and are due to the differences in the radiative and thermal properties of concrete structures and foliated regions. On the average, the urban heat island temperature pattern shows that the maximum temperature is found in the structure regions of the city; the temperature decreases rather uniformly away from this region to a minimum temperature in the surrounding suburban or agricultural regions. However, if a body of water characterizes part of the peripheral regions, a near discontinuity in the temperature gradient will exist which usually is found right at the boundary between the city and the body of water (Findlay and Hirt 1969). For cities isolated from bodies of water, the thermal pattern associated with the urban heat island departs from that of the classical heat island in that no discontinuities are evident in the temperature gradients.

The urban heat island exhibits a marked diurnal oscillation (Mitchell 1961). The largest contrast between the structure regions of the city and the suburban area is at night, and little or no contrast exists during daylight hours. At night, there is a significant difference between the vertical temperature distributions in the suburban and urban regions. Examples given by Clarke (1969) indicate that the boundary layer is less stable in the city.

The urban heat island, though not as abrupt a perturbation as the classical heat island, should produce a solenoidal circulation similar to the sea breeze circulation. The basic principle under which the urban heat island circulation is produced is the same as the sea breeze circulation; only the character of the forcing function is different. The differential heating between the city and the suburban areas would set up a mass and thermal contrast. The available potential energy is converted into kinetic energy through warm air rising and cold air sinking. A heat Low and horizontal convergence would characterize the heated zone; and horizontal divergence would be found in the cooling zone (Stern and Malkus 1963; Smith 1955, 1957). The differential heating also produces a gravity wave train which is propagated upstream and downstream and produces oscillations on the basic solenoid circulation (Geisler and Bretherton 1969).

There has been only scattered evidence that such a circulation exists. Findlay and Hirt (1969) investigated the mesoscale flow pattern in Toronto, Canada. The flow was associated with the urban heat island, but the proximity of Lake Ontario and the large temperature gradient at the boundary of the lake and city would indicate that the lake breeze also played an important role in the mesoscale meteorology of this city. Separation of the components of the circulation due to the lake breeze and the heat island was not possible. The total effect was to produce an inflow to the city with speeds as large as 1.71 m/s.

Models of the classical heat island circulation indicate a rather strong wind system should be present (Tanouye 1966, Estoque and Bhumralkar 1969). However, these models have near-infinite temperature gradients between the heated and unheated regions. Under these circumstances, strong winds are to be expected. In this paper, a simple linear model is used to compute the wind system associated with a heating distribution more characteristic of the urban heat island. The heating distribution used would produce a smoothly varying temperature field with a maximum temperature in the center of the city, which is assumed to be the built up region, and a minimum temperature in the peripheral regions. The maximum temperature gradient would be found at the boundary between the city and surburban regions, and the temperature gradient is continuous. A linear friction term is introduced in the model, and the coefficient of friction is assumed independent of space and time. The model

describes the flow for two stability categories: (1) a stable boundary layer and (2) a relatively unstable boundary layer. Each of these stability categories are described for a no-mean-wind case and for the case when a mean wind existed. The mean wind was assumed independent of space and time.

2. MODEL I (NO-MEAN WIND)

The heating, and therefore motion, was constrained to vary along the x- and the z-coordinates. This defines an infinitely long heat mound along the y-coordinate. Because the time and space scales associated with the urban heat island circulation are small, the Coriolis force can be neglected. Under the above constraints, the linearized perturbation equations of motion for the case of no-mean wind are simply

$$\frac{\partial u'}{\partial t}+Ku'=-\frac{1}{\bar{\rho}}\frac{\partial p'}{\partial x}$$

and

$$\frac{\partial w'}{\partial t}+Kw'=-\frac{1}{\bar{\rho}}\frac{\partial p'}{\partial z}-\frac{\rho'}{\bar{\rho}}g \tag{1}$$

where u' is the perturbation x-wind component, t is time, p' is the perturbation pressure, $\bar{\rho}$ is the average density independent of t and x, w' is the perturbation vertical velocity, g is gravity, K is the coefficient of friction, and ρ' is the perturbation density. Cross differentiation and subtraction of the equations of motion lead to the perturbation vorticity equation

$$\left(\frac{\partial}{\partial t}+K\right)\left(\frac{\partial u'}{\partial z}-\frac{\partial w'}{\partial x}\right)+\frac{\partial \beta}{\partial x}=0 \tag{2}$$

where β is $-\rho' g/\bar{\rho}=\theta' g/\bar{\theta}$, θ' is the perturbation potential temperature, and $\bar{\theta}$ is the average potential temperature independent of t and x. Assuming nondivergence, a stream function, ψ, can be found such that $u'=\partial\psi/\partial z$ and $w'=-\partial\psi/\partial x$; and eq (2) becomes

$$\left(\frac{\partial}{\partial t}+K\right)\left(\frac{\partial^2\psi}{\partial z^2}+\frac{\partial^2\psi}{\partial x^2}\right)+\frac{\partial \beta}{\partial x}=0. \tag{3}$$

The model is such that horizontal variations of the vertical motions are much smaller than vertical variations of the horizontal motions (i.e., $\partial^2\psi/\partial z^2 >> \partial^2\psi/\partial x^2$). This is essentially the same as assuming hydrostatic equilibrium. Therefore,

$$\left(\frac{\partial}{\partial t}+K\right)\frac{\partial^2\psi}{\partial z^2}+\frac{\partial \beta}{\partial x}=0. \tag{4}$$

The diurnal temperature curves in urban areas and their peripheral zones indicate that the temperature contrast between these areas begins to increase at around mid-afternoon (Mitchell 1961, Clarke 1969, Peterson 1969). At this time, the data show that the temperature is decreasing in both regions, or there is general cooling occurring. However, the surrounding areas are cooling at a more rapid rate. To describe this form of the heating function, the heat energy added per unit time and mass was assumed to be composed of two parts: (1) an average heating rate, $\bar{Q}$, independent of t and x and (2) a superimposed heating perturbation. The perturbation heating function was independent of time. Both the average heating and the perturbation heating were allowed to persist in the boundary layer from the ground to a level $z=h$. Above $z=h$, heating was everywhere zero. The heating function is

$$Q=(\bar{Q}+Q'\cos kx)H(h-z)$$

where Q is the heating rate, Q' is the amplitude of the perturbation heating rate, $H(h-z)$ is the Heaviside unit function (Pipes 1958), and k is the spatial wave number for the heat perturbation. Since $\bar{Q}<0$ and $|\bar{Q}|>|Q'|$, the above function would describe a cooling distribution that would produce the tendencies observed in the diurnal temperature data.

The first law of thermodynamics may be written in linearized form and, under the constraints given above, in the following manner:

$$\frac{\partial \beta}{\partial t}-\omega^2\frac{\partial \psi}{\partial x}=(\lambda\cos kx)H(h-z) \tag{5}$$

where ω^2 is $(g/\bar{\theta})(\partial\bar{\theta}/\partial z)$ and λ is $Q'g/\bar{\theta}$. Eliminating β from eq (4) and (5) yields

$$\left(\frac{\partial^2}{\partial t^2}+K\frac{\partial}{\partial t}\right)\frac{\partial^2\psi}{\partial z^2}+\omega^2\frac{\partial^2\psi}{\partial x^2}=\lambda k H(h-z)\sin kx. \tag{6}$$

Equation (6) is the governing equation that describes the motion. The solution of this equation was found by separation of variables and subject to the boundary conditions

$$\psi=0,\ z=0,\ t\geq 0,$$
$$\psi=0,\ z=D,\ t\geq 0,$$

and

$$\psi=\frac{\partial\psi}{\partial t}=0,\ z\geq 0,\ t=0 \tag{7}$$

where D corresponds to the top of the layer influenced by the urban heat island and acts as a rigid lid. Letting

$$\lambda H(h-z)=\omega^2(z)\sum_{p=0}^{\infty}A_p\xi_p(z) \tag{8}$$

and

$$\psi=\sum_{p=0}^{\infty}f_p(x,t)\xi_p(z) \tag{9}$$

where A_p, the amplitude term in the series, is

$$A_p=\int_0^h \xi_p(z)dz\left[\int_0^D \omega^2(z)\xi_p^2(z)dz\right]^{-1}, \tag{10}$$

p is the index used in the summations ($p=1, 2, 3, \ldots$), ξ_p and f_p are functions of z and of x and t, respectively, and are to be determined.

Substituting eq (8) and (9) into eq (6) yields

$$\frac{\partial^2\xi_p}{\partial z^2}+\frac{\omega^2}{c_p^2}\xi_p=0 \tag{11}$$

and

$$\frac{\partial^2 f_p}{\partial t^2}+K\frac{\partial f_p}{\partial t}-c_p^2\frac{\partial^2 f_p}{\partial x^2}=-A_p k c_p^2 \sin kx \tag{12}$$

where c_p is the separation constant and is the wave speed. Solution of eq (12) takes the form

$$f_p=g(t)\sin kx+r(t)\cos kx \tag{13}$$

provided

$$\frac{\partial^2 g}{\partial t^2}+K\frac{\partial g}{\partial t}+k^2c_p^2 g=-A_p k c_p^2 \tag{14}$$

and

$$\frac{\partial^2 r}{\partial t^2}+K\frac{\partial r}{\partial t}+k^2c_p^2 r=0. \tag{15}$$

The boundary conditions [eq (7)] yield $r(t)=0$ and

$$g(t)=-\frac{A_p}{k}\left\{1-\frac{c_p k}{\sqrt{c_p^2k^2-\left(\frac{K}{2}\right)^2}}\times\exp\left(-\frac{K}{2}t\right)\sin\left[\sqrt{c_p^2k^2-\left(\frac{K}{2}\right)^2}\,t+\phi\right]\right\} \tag{16}$$

where ϕ is arctan $[\sqrt{c_p^2k^2-(K/2)^2}/(K/2)]$. This gives the partial solution

$$f_p=-\frac{A_p}{k}\left\{1-\frac{c_p k}{\sqrt{c_p^2k^2-\left(\frac{K}{2}\right)^2}}\times\exp\left(-\frac{K}{2}t\right)\sin\left[\sqrt{c_p^2k^2-\left(\frac{K}{2}\right)^2}\,t+\phi\right]\right\}\sin kx. \tag{17}$$

This solution corresponds to a forced response associated with the heating distribution and a damped transient response associated with gravity waves produced by heating.

The solution of eq (11) is dependent on ω which varies in the vertical as $\bar{\theta}$ varies. For this study, the atmosphere was assumed to be characterized by essentially two stability layers; that is,

$$\omega=\omega_1 \quad 0\le z\le h\text{—the boundary layer}$$

and

$$\omega=\omega_2 \quad h\le z\le D$$

where $(\partial \ln\bar{\theta}/\partial z)$ is a constant in each layer. Under these conditions, the solution that satisfies the boundary conditions [eq (7)] and the continuity conditions

$$\left.\begin{aligned}\xi_{1p}&=\xi_{2p}\\ \frac{\partial\xi_{1p}}{\partial z}&=\frac{\partial\xi_{2p}}{\partial z}\end{aligned}\right\} z=h$$

is

$$\xi_{1p}=\sin\left(\frac{\omega_1 z}{c_p}\right), \qquad 0\le z\le h \tag{18}$$

and

$$\xi_{2p}=\sin\left(\frac{\omega_1 h}{c_p}\right)\sin\left[\frac{\omega_2}{c_p}(z-D)\right]\sin^{-1}\left[\frac{\omega_2}{c_p}(h-D)\right],\ h\le z\le D$$

provided

$$\omega_1\cot\left(\frac{\omega_1 h}{c_p}\right)+\omega_2\cot\left[\frac{\omega_2}{c_p}(D-h)\right]=0. \tag{19}$$

Solution of eq (19) yields the eigenvalues c_p. Equation (18) together with eq (10) gives the amplitude term, A_p; that is,

$$A_p=\frac{2c_p\lambda}{\omega_1\omega_2^2}\left[1-\cos\left(\frac{\omega_1 h}{c_p}\right)\right]\times\left\{\left(\frac{\omega_1}{\omega_2}\right)^2 h+(D-h)\frac{\sin^2\left(\frac{\omega_1 h}{c_p}\right)}{\sin^2\left[\frac{\omega_2}{c_p}(h-D)\right]}\right\}^{-1}. \tag{20}$$

Therefore, the complete solution to eq (6) is

$$\psi=\sum_{p=1,\,c_p}^{p=n}\left(-\frac{2c_p\lambda}{k\omega_2^2\omega_1}\right)\left\{1-\frac{c_p k}{\sqrt{c_p^2k^2-\left(\frac{K}{2}\right)^2}}\times\exp\left(-\frac{K}{2}t\right)\sin\left[\sqrt{c_p^2k^2-\left(\frac{K}{2}\right)^2}\,t+\phi\right]\right\}\times(\sin kx)\left[1-\cos\left(\frac{\omega_1 h}{c_p}\right)\right]\left\{\left(\frac{\omega_1}{\omega_2}\right)^2 h+\frac{(D-h)\sin^2\left(\frac{\omega_1 h}{c_p}\right)}{\sin^2\left[\frac{\omega_2}{c_p}(h-D)\right]}\right\}^{-1}\times\begin{bmatrix}\sin\left(\frac{\omega_1 z}{c_p}\right) & 0\le z\le h\\ \sin\left(\frac{\omega_1 h}{c_p}\right)\sin\left[\frac{\omega_2}{c_p}(z-D)\right]\sin^{-1}\left[\frac{\omega_2}{c_p}(h-D)\right] & h\le z\le D\end{bmatrix} \tag{21}$$

where the summation is over the eigenvalues determined through the solution of eq (19), and the summation is over a finite interval because it converges rapidly as c_p becomes small.

The solutions of eq (19) and (21) were found for two stability categories in the lowest layer ($0\le z\le h$). In the upper layer, the standard atmospheric lapse rate was used to compute ω_2 for both cases. The lower layer was characterized by an isothermal layer in one case ($\partial T/\partial z=0$) and a near-neutral stratification in the other ($\partial T/\partial z=-8.0$°C/km). The top of the atmosphere was assumed to be the 10-km level (i.e., $D=10$ km), and the top of the layer in which the urban heat island is found was 1 km (i.e., $h=1.0$ km). The heating amplitude, λ, was determined from data on the temperature distribution associated with heat islands of various cities and from the diurnal variation of temperature in cities and in adjacent surroundings. The value used was such that a 6°C temperature difference would exist between the center of the city (center of maximum relative heating) and a point 20 km away (center of relative maximum cooling) in 3 hr. This is a relatively strong urban heat island. The maximum temperature gradient would be found at the boundary

between the city and surroundings which is approximately 10 km from the center of the city. The coefficient of friction was assumed to be $10^{-4}s^{-1}$ for both cases even though the difference in stabilities should produce a larger coefficient for the near-neutral case. The variations produced by having different coefficients of friction were not of any consequence in the model, and can be inferred easily from the given results.

The solution of eq (21) under the above specifications yielded numerous qualitative similarities between the case of a near-neutral and a stable boundary layer. A two-cell circulation system characterized both cases. Low-level horizontal convergence, upward vertical motions, and upper level horizontal divergence describe the motion field over the city. Low-level horizontal divergence, downward vertical motion, and upper level horizontal convergence, describe the motion field in the surrounding areas.

As the similarities are obvious, so are the dissimilarities. Figures 1 and 2 yield the horizontal wind speed profile at $x=10$ km which is the point of maximum temperature gradient and maximum horizontal wind speed for the stable and near-neutral cases, respectively. The figures show the wind speed in the 0.5- and 1.5-hr time frames. For positive x directions, positive wind speeds indicate flow away from the city and negative wind speeds, flow to the city. The horizontal wind speeds are greater for the stable case. Maximum low-level wind for the stable case is approximately 0.8 m/s as opposed to 0.32 m/s for the near-neutral case. The vertical extent of the circulation is larger for the near-neutral case (approx. 4.0 km) than for the stable case (approx. 1.5 km).

Vertical convection should be greater for the near-neutral case than for the stable case. The vertical compression associated with the stable case requires larger horizontal velocities to maintain the nondivergent state assumed. On the other hand, the vertical velocities would be larger for the near-neutral case. Figures 3 and 4 show the profile of the vertical velocities for the two cases located in the center of the city ($x=0$) where the maximum vertical velocity was found. The maximum vertical wind speed for the stable case was approximately 5.0 cm/s and for the near-neutral case, 5.7 cm/s. The differences in the vertical extent of the vertical velocities reflect the differences in the depths of the circulation.

The variation in time depicted in figures 1 through 4 reflects the effect of the transient response associated with propagating gravity waves. Friction damped this effect so that after 3 hr, the solution reached a steady state which was very near the 0.5-hr solution.

These calculations suggest that horizontal wind speeds associated with the urban heat island circulation are small, and that the circulation would be strongest at night when the boundary layer is stable. Statistical evidence indicates that the urban heat island is strongest at night. Therefore, the circulation has the highest probability of detection at that time. On the other hand, the vertical wind speeds are significant for both cases. There is a good possibility that the circulation could enhance

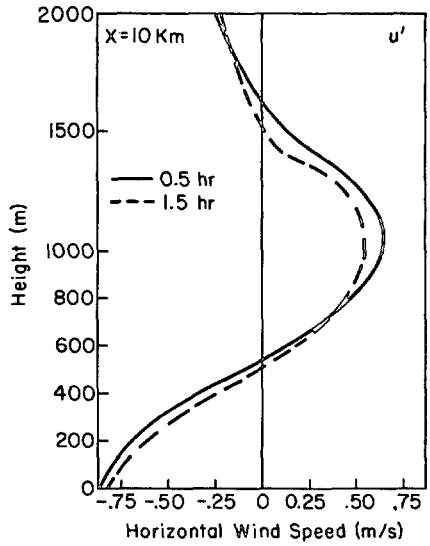

FIGURE 1.—Vertical profile of horizontal wind speed for the stable case ($\partial T/\partial z=0$) at $x=10$ km.

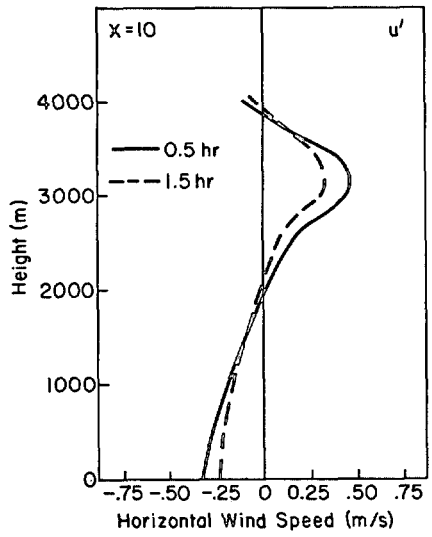

FIGURE 2.—Vertical profile of horizontal wind speed for the near-neutral case ($\partial T/\partial z=-8°C/km$) at $x=10$ km.

cumulus production provided the required moisture is present. It could also act as a ventilation factor removing air pollutants by vertical convection. Though this calculation yields a closed circulation system which therefore could not ventilate at all, the reality of this result is questionable because the assumption of no-mean wind in the upper levels is highly improbable. Nonlinear interaction between the mean state and the perturbation state would allow removal of the pollutants. However, a mean wind produces another interesting effect which is described in the next section.

3. MODEL II (MEAN WIND ADDED)

In deriving the equations govening the motion for this case, all conditions specified in section 2 hold except that

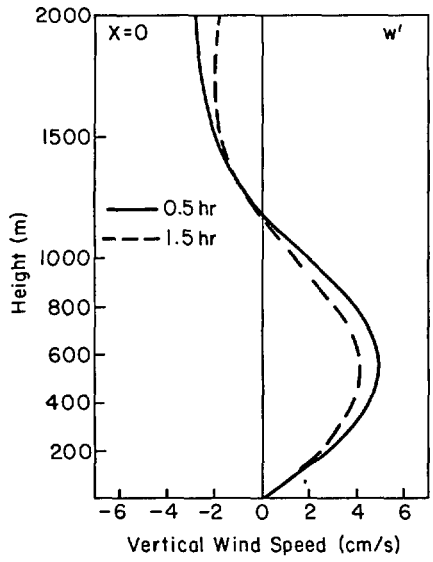

FIGURE 3.—Vertical profile of vertical wind speed for the stable case ($\partial T/\partial z=0$) at $x=0$.

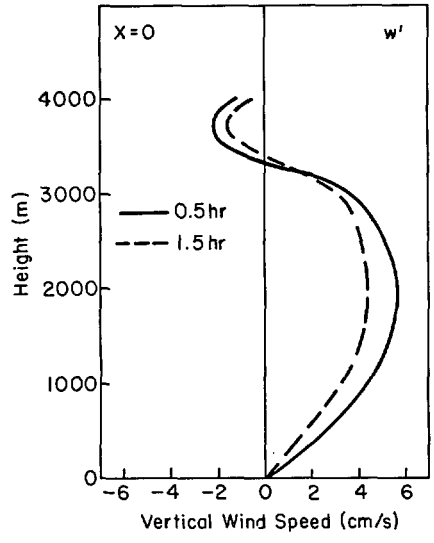

FIGURE 4.—Vertical profile of vertical wind speed for the near-neutral case ($\partial T/\partial z=-8°$C/km) at $x=0$.

friction was neglected and the mean wind, $\overline{U}$, was assumed to be independent of x, z, and t. The equations of motion are

$$\left(\frac{\partial}{\partial t}+\overline{U}\frac{\partial}{\partial x}\right)u'=-\frac{1}{\bar{\rho}}\frac{\partial p'}{\partial x}$$

and (22)

$$\left(\frac{\partial}{\partial t}+\overline{U}\frac{\partial}{\partial x}\right)w'=-\frac{1}{\bar{\rho}}\frac{\partial p'}{\partial z}+\beta.$$

Following the procedure described in section 2, the vorticity equation derived for this case is

$$\left(\frac{\partial}{\partial t}+\overline{U}\frac{\partial}{\partial x}\right)\frac{\partial^2\psi}{\partial z^2}+\frac{\partial\beta}{\partial x}=0; \tag{23}$$

and the thermodynamic equation is

$$\left(\frac{\partial}{\partial t}+\overline{U}\frac{\partial}{\partial x}\right)\beta-\omega^2\frac{\partial\psi}{\partial x}=(\lambda\cos kx)\,H(h-z). \tag{24}$$

Eliminating β from eq (23) and (24) yields

$$\left(\frac{\partial}{\partial t}+\overline{U}\frac{\partial}{\partial x}\right)^2\frac{\partial^2\psi}{\partial z^2}+\omega^2\frac{\partial^2\psi}{\partial x^2}=\lambda kH(h-z)\sin kx. \tag{25}$$

The technique used to solve eq (25) is identical to that used to solve eq (6). Substituting eq (8) and (9) into eq (25) yields

$$\left(\frac{\partial}{\partial t}+\overline{U}\frac{\partial}{\partial x}\right)^2 f_p-c_p^2\frac{\partial^2 f_p}{\partial x^2}=-A_pkc_p^2\sin kx \tag{26}$$

and

$$\frac{\partial^2\xi_p}{\partial z^2}+\frac{\omega^2}{c_p^2}\xi_p=0. \tag{27}$$

the solution to eq (27) is identical to that in section 2, and the solution to eq (26) was found in the following manner. The solution is identical to eq (13) provided

$$\frac{\partial^2 g}{\partial t^2}-2\overline{U}k\frac{\partial r}{\partial t}-k^2(\overline{U}^2-c_p^2)g=-A_pc_p^2k \tag{28}$$

and

$$\frac{\partial^2 r}{\partial t^2}+2\overline{U}k\frac{\partial g}{\partial t}-k^2(\overline{U}^2-c_p^2)r=0. \tag{29}$$

Simultaneous solution of these equations yields:

$$\left[\frac{\partial^4}{\partial t^4}+2k^2(\overline{U}^2+c_p^2)\frac{\partial^2}{\partial t^2}+k^4(\overline{U}^2-c_p^2)^2\right]g=A_pc_p^2k^3(\overline{U}^2-c_p^2) \tag{30}$$

and

$$\left[\frac{\partial^4}{\partial t^4}+2k^2(\overline{U}^2+c_p^2)\frac{\partial^2}{\partial t^2}+k^4(\overline{U}^2-c_p^2)^2\right]r=0. \tag{31}$$

The boundary conditions [eq (7)] and eq (28) and (29) provided two additional boundary conditions which are required to solve eq (30) and (31):

$$\frac{\partial^2 g}{\partial t^2}=-A_pc_p^2k,\qquad \frac{\partial^2 r}{\partial t^2}=0,\qquad t=0$$

and (32)

$$\frac{\partial^3 g}{\partial t^3}=0,\qquad \frac{\partial^3 r}{\partial t^3}=2A_pc_p^2k^2\overline{U},\qquad t=0.$$

Solutions of eq (30) and (31) are, respectively,

$$g(t)=\frac{A_p}{k}\left(\frac{c_p}{\overline{U}^2-c_p^2}\right)\left\{c_p+\left(\frac{\overline{U}-c_p}{2}\right)\cos[k(\overline{U}+c_p)t]-\left(\frac{\overline{U}+c_p}{2}\right)\cos[k(\overline{U}-c_p)t]\right\} \tag{33}$$

and

$$r(t)=\frac{A_p}{k}\left(\frac{c_p}{\overline{U}^2-c_p^2}\right)\left\{\left(\frac{\overline{U}+c_p}{2}\right)\sin[k(\overline{U}-c_p)t]-\left(\frac{\overline{U}-c_p}{2}\right)\sin[k(\overline{U}+c_p)t]\right\}. \tag{34}$$

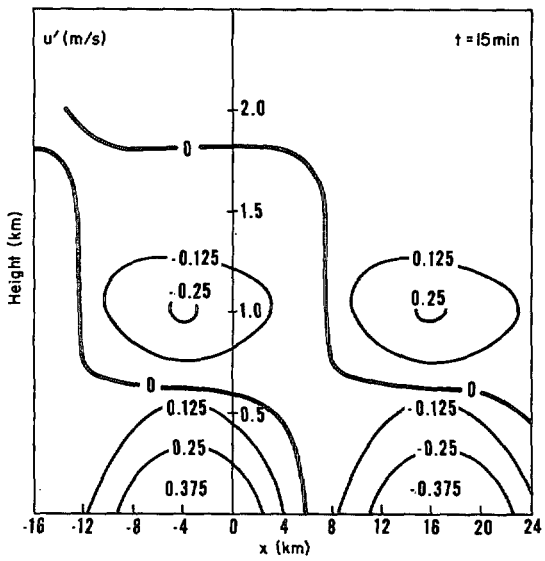

FIGURE 5.—Vertical and horizontal distribution of horizontal wind speed for the stable case ($\partial T/\partial z=0$, $\bar{U}=10$ m/s) after 15 min.

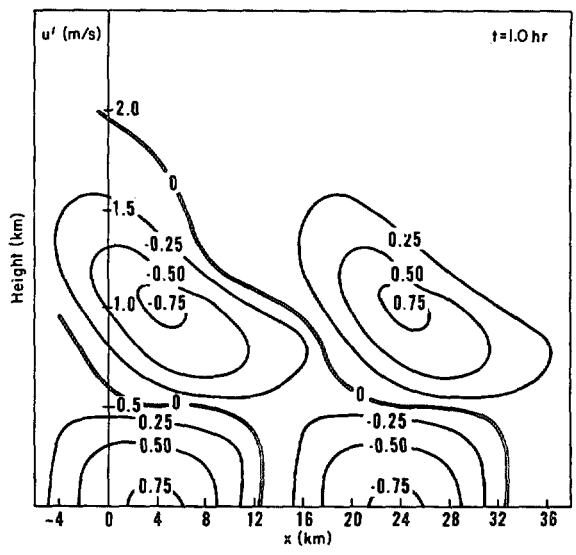

FIGURE 7.—Vertical and horizontal distribution of horizontal wind speed for the stable case ($\partial T/\partial z=0$, $\bar{U}=10$ m/s) after 1 hr.

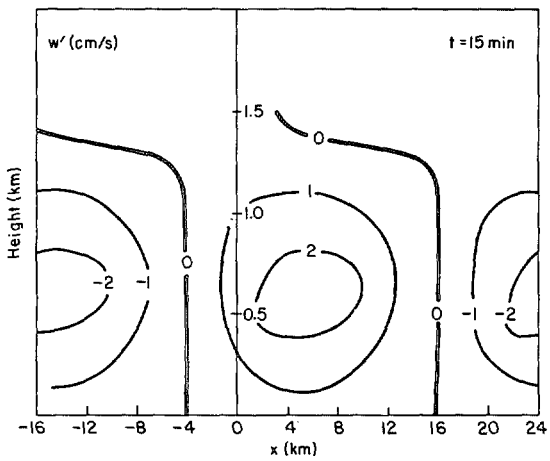

FIGURE 6.—Vertical and horizontal distribution of vertical wind speed for the stable case ($\partial T/\partial z=0$, $\bar{U}=10$ m/s) after 15 min.

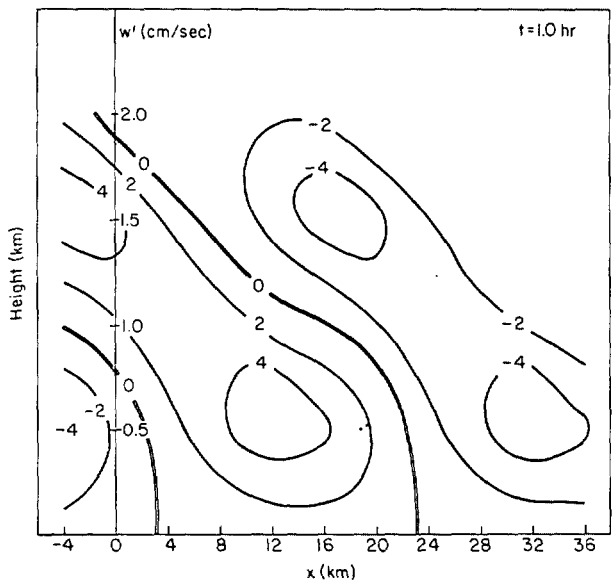

FIGURE 8.—Vertical and horizontal distribution of vertical wind speed for the stable case ($\partial T/\partial z=0$, $\bar{U}=10$ m/s) after 1 hr.

The part of the solution acquired for eq (15) in section 2 was $r(t)=0$ which fixed the spatial phase angle of the streamline pattern for all time. However, in this problem, $r(t)\neq 0$ so that the streamline pattern will be displaced in space, and the displacement is time dependent. This is brought about by advection of heat and momentum by the mean wind.

Equations (9), (13), (18), (19), (20), (33), and (34) were combined to obtain the velocity fields for this case. Parameters described in section 2 were used to solve the equations. The mean wind speed was assumed to be 10 m/s and was positive (i.e., air motions are toward the increasing x-direction).

Figure 5 yields the distribution of the horizontal wind after 15 min for the stable case. The two-cell circulation system is evident in the horizontal velocity field on the entire system and is displaced 6 km in the positive x-direction from the heat source ($x=0$); that is, the zone of low-level convergence is found at approximately $x=6$ km. The vertical extent of the circulation has increased by about 250 m from the no-mean-wind case (sec. 2). The horizontal velocities are small because it is early in the integration period. Figure 6 shows the vertical velocity distribution corresponding to figure 5. The region of maximum upward motion which was found at $x=0$ in the no-mean-wind case has moved to $x=6$ km in correspondence to the effect of the mean wind. The peripheral regions of the city show regions of downward vertical motions.

Figure 7 shows the horizontal velocity distribution after 1 hr for the stable case. The circulation system has reached the intensity observed in the no-mean-wind case, but it is displaced approximately 12 km from the heat source in the positive x-direction. The circulation did not move beyond this position for the next 1 to 2 hr, though

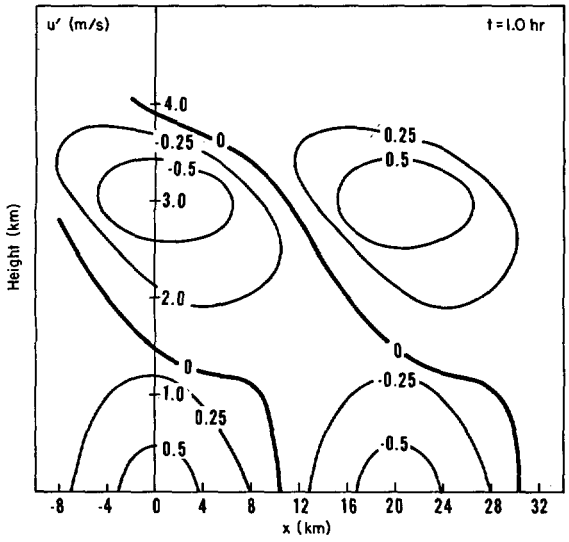

FIGURE 9.—Vertical and horizontal distribution of horizontal wind speed for the near-neutral case ($\partial T/\partial z = -8°C/km$) and for $\bar{U} = 10$ m/s after 1 hr.

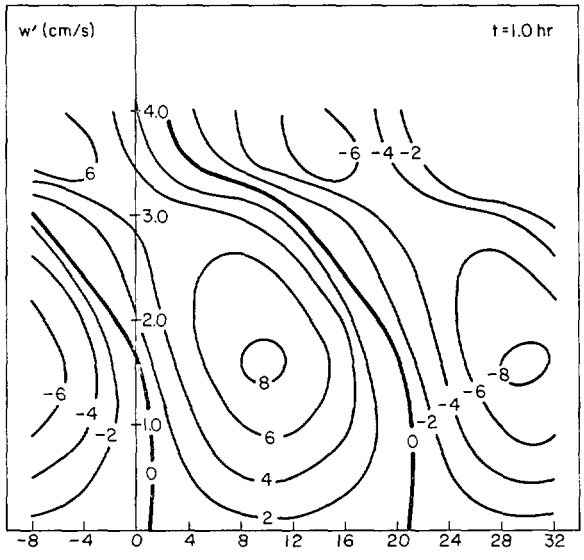

FIGURE 10.—Vertical and horizontal distribution of vertical wind speed for the near-neutral case ($\partial T/\partial z = -8°C/km$) and for $\bar{U} = 10$ m/s after 1 hr.

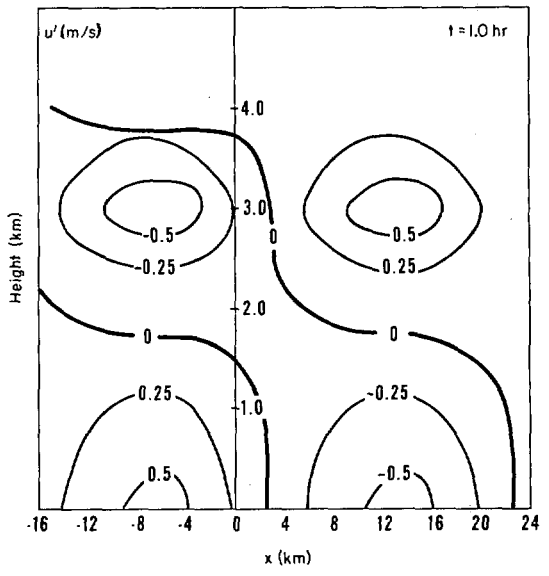

FIGURE 11.—Vertical and horizontal distribution of horizontal wind speed for the near-neutral case ($\partial T/\partial z = -8°C/km$) and for $\bar{U} = 3$ m/s after 1 hr.

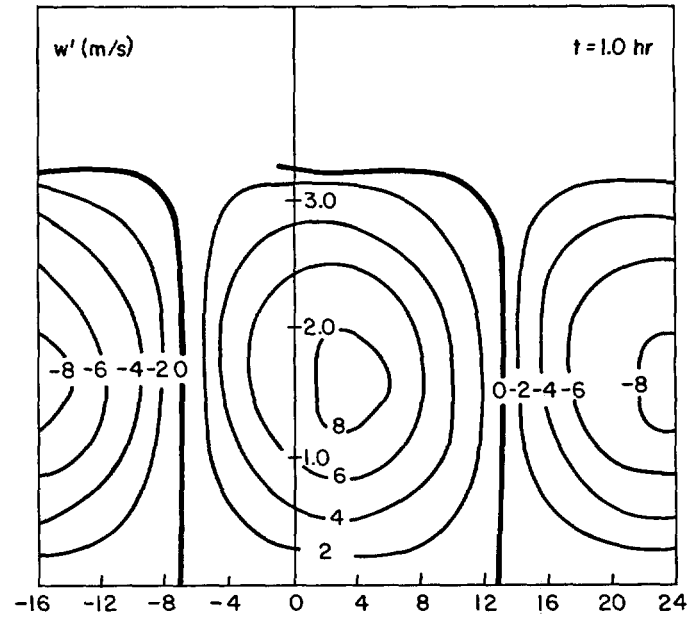

FIGURE 12.—Vertical and horizontal distribution of vertical wind speed for the near-neutral case ($\partial T/\partial z = -8°C/km$) and for $\bar{U} = 3$ m/s after 1 hr.

the intensity varied, reflecting the effect of the transient gravity wave response. The speed of the circulation system is influenced by the mean wind speed, the gravity wave speed, and the heating distribution. The quasi-equilibrium state for the system is brought about by a momentary balance between the acceleration produced by the heating distribution tending to bring the system back to the heat source and the mean wind and gravity wave effects which transport heat and momentum downstream [Vukovich and Chow (1968)]. Afterwards it continued its displacement downstream.

The vertical velocity field (fig. 8) shows approximately the same intensity obtained for the no-mean-wind case and also demonstrates the displacement of the circulation system. It is interesting to note that the center of the heat source, which is considered the center of the city, is characterized by downward vertical motions. This result also was obtained by Estoque and Bhumralkar (1969). Whereas the heat island circulation might act as an urban ventilator under the no-mean-wind case, when there is a mean wind that displaces the circulation downstream the downward vertical motions that characterize the larger part of the city would prevent any large magnitude exchange in the vertical.

Figures 9 and 10 yield the horizontal and vertical velocity distribution for the near-neutral case after 1 hr. The systems remain stationary. The intensity and the vertical extent of the horizontal circulation is about equal

to that found for the no-mean-wind case, but the system is displaced downstream 11 km. The vertical velocity field, on the other hand, is more intense and also exhibits the 11-km displacement. As in the stable case, the center of the city is characterized by downward vertical motions.

The effect of using a different mean wind speed can be determined by comparing figures 9 and 10 with figures 11 and 12. Figures 11 and 12 yield the horizontal and vertical velocity distributions, respectively, for the near-neutral case after 1 hr and for a mean wind of 3 m/s. The main difference between the two cases is a matter of system displacement. The system was displaced only about 3 km when $\bar{U}=3$ m/s.

4. SUMMARY AND CONCLUSIONS

Differential heating between the urban complex and the peripheral environs produces the urban heat island. The same differential heating produces the heat island circulation, and the intensity of the circulation is dependent on the amplitude and scale of the heat differential. Diurnal variations in the temperature difference between the city and suburbs indicate that the heat island is most intense at night and least intense during the day. There are situations when during the day the surrounding environment is warmer than the city. These data show that in the midafternoon, the contrast between the city and suburbs begins to increase. At the same time, both regions are cooling. Though the mean effect is cooling, the cooling rate is larger in the suburbs than in the city. The result is to establish a temperature gradient from city to suburb.

The differential heating distribution produces a weak two-cell circulation system with low-level horizontal convergence, upward vertical motions, and upper level horizontal divergence over the city, and low-level horizontal divergence, downward vertical motions, and upper level horizontal divergence over the suburbs when there is no mean wind. When a mean wind exists, the circulation system is displaced downstream a distance that appears to be proportional to the mean wind speed and the heating rate. The speed of the system is governed by the mean wind speed, gravity wave speed, and the heating distribution. At a certain point, the acceleration produced by the heating distribution, tending to bring the circulation back to the heat source, is balanced by convective transport of heat and momentum by the mean wind so that the system becomes stationary. This state persists for about 1 to 2 hr.

Normally, the boundary layer is near neutral or unstable in the early afternoon, so that the circulation would have a large vertical extent in its incipient stage. The horizontal motions would be small, but the vertical velocities can be reasonably large. As night approaches, the boundary layer becomes more stable, and the vertical dimensions of the system decrease. The horizontal speeds increase, and the vertical speeds decrease. The most intense horizontal speeds of the urban heat island circulation would be experienced in the stable nighttime state, but the most intense vertical motions would be found in the early afternoon when the boundary layer is less stable.

These results lead to some interesting possibilities. During the early and midafternoon hours, when the vertical speeds are most intense and exist through a relatively deep layer, the urban heat island circulation could help enhance cloud development. The circulation systems also may help ventilate the city. However, if a large mean wind exists, the zone of upward vertical motions would be displaced downstream, and downward vertical motions could characterize the urban regions, suppressing vertical transports of pollutants. Under this condition, any cumulus development would be enhanced by the circulation downstream of the urban complex.

ACKNOWLEDGMENT

The author expresses his appreciation to Donna Nifong for her computer programming effort.

REFERENCES

Clarke, John F., "Nocturnal Urban Boundary Layer Over Cincinnati, Ohio," *Monthly Weather Review*, Vol. 97, No. 8, Aug. 1969, pp. 582–589.

Estoque, M. A., and Bhumralkar, C. M., "Flow Over a Localized Heat Source," *Monthly Weather Review*, Vol. 97, No. 12, Dec. 1969, pp. 850–859.

Findlay, B. F., and Hirt, M. S., "An Urban-Induced Meso-Circulation," *Atmospheric Environment*, Vol. 3, No. 5, Pergamon Press, Oxford, England, Sept. 1969, pp. 537–542.

Geisler, J. E., and Bretherton, F. P., "The Sea-Breeze Forerunner," *Journal of the Atmospheric Sciences*, Vol. 26, No. 1, Jan. 1969, pp. 82–95.

Lowry, William P., "The Climate of Cities," *Scientific American*, Vol. 217, No. 2, New York, N.Y., Aug. 1967, pp. 15–23.

Malkus, Joanne Starr, and Stern, Melvin E., "The Flow of a Stable Atmosphere Over a Heated Island, Part I," *Journal of Meteorology*, Vol. 10, No. 1, Feb. 1953, pp. 30–41.

Mitchell, J. Murray, Jr., "The Thermal Climate of Cities," *Symposium on Air Over Cities, Cincinnati, Ohio, November 6–7, 1961*, U.S. Public Health Service Report No. AG2–5, Cincinnati, Ohio, Nov. 1961, pp. 131–145.

Peterson, James T., "The Climate of Cities: A Survey of Recent Literature," *National Air Pollution Control Administration Publication* No. AP–59, Raleigh, N.C., Oct. 1969, 48 pp.

Pipes, L. A., *Applied Mathematics for Engineers and Physicists* 2d edition, McGraw-Hill Book Co., Inc., New York, N.Y., 1958, 723 pp.

Smith, Ralph C., "Theory of Air Flow Over a Heated Land Mass," *Quarterly Journal of the Royal Meteorological Society*, Vol. 81, No. 349, London, England, July 1955, pp. 382–395.

Smith, Ralph C., "Air Motion Over a Heated Land Mass, Pt. 2," *Quarterly Journal of the Royal Meteorological Society*, Vol. 83, No. 356, London, England, Apr. 1957, pp. 248–256.

Tanouye, E. T., "The Response of the Atmosphere to a Localized Heat Source at the Earth's Surface," *Final Report*, Grant No. DA–AMC–28–043–64–G–2, Hawaii Institute of Geophysics, Honolulu, Aug. 1966, pp. 123–171.

Vukovich, Fred M., and Chow, C. F., "Research in Numerical, Dynamical, and Operational Weather Forecast Procedures," *Final Report*, Contract No. AF19(628)–5834, Air Force Cambridge Research Laboratories, Bedford, Mass., Apr. 1968, 89 pp.

[Received February 24, 1971; revised April 16, 1971]